Critical roles of Rad54 in tolerance to apigenin-induced Top1-mediated DNA damage

ZILU ZHAO[1*], XIAOHUA WU[2*], FANG HE[2*], CUIFANG XIANG[1], XIAOYU FENG[1], XIN BAI[1], XIN LIU[1], JINGXIA ZHAO[1], SHUNICHI TAKEDA[3] and YONG QING[1]

[1]Department of Pharmacology, Key Laboratory of Drug-Targeting and Drug Delivery Systems of the Education Ministry, West China School of Pharmacy, Sichuan University, Chengdu, Sichuan 610041; [2]State Key Laboratory of Biotherapy and Cancer Center, West China Hospital, Sichuan University, Chengdu, Sichuan 610041, P.R. China; [3]Department of Radiation Genetics, Graduate School of Medicine, Kyoto University, Kyoto 606-8501, Japan

Received December 12, 2019; Accepted July 7, 2020

DOI: 10.3892/etm.2021.9936

Abstract. Apigenin (APG), a flavone sub-class of flavonoids, possesses a diverse range of biological activities, including anti-cancer and anti-inflammatory effects. Previous studies identified the genotoxicity of APG in certain cancer cells, which may be associated with its anticancer effect. However, the DNA damage repair mechanism induced by APG has remained elusive. In order to clarify the molecular mechanisms, the present study determined the toxicity of APG to the wild-type (*WT*) DT40 chicken B-lymphocyte cell line, as well as to DT40 cells with deletions in various DNA repair genes, and their sensitivities were compared. It was demonstrated that cells deficient of Rad54, a critical homologous recombination gene, were particularly sensitive to APG. Cell-cycle analysis demonstrated that APG caused an increase in the G_2/M-phase population of *Rad54*$^{-/-}$ cells that was greater than that in *WT* cells. Furthermore, it was demonstrated by immunofluorescence assay that *Rad54*$^{-/-}$ cells exhibited significantly increased numbers of γ-phosphorylated H2AX variant histone foci and chromosomal aberrations compared to the *WT* cells in response to APG. Of note, the *in vitro* complex of enzyme assay indicated that APG induced increased topoisomerase I (Top1) covalent protein DNA complex in *Rad54*$^{-/-}$ cells compared to *WT* cells. Finally, these results were verified using the TK6 human lymphoblastoid cell line and it was demonstrated that, as for DT40 cells, Rad54 deficiency sensitized TK6 cells to APG. The present study demonstrated that Rad54 was involved in the repair of APG-induced DNA damage, which was associated with Top1 inhibition.

Correspondence to: Professor Yong Qing, Department of Pharmacology, Key Laboratory of Drug-Targeting and Drug Delivery Systems of the Education Ministry, West China School of Pharmacy, Sichuan University, 17 Section, 3 People's South Road, Chengdu, Sichuan 610041, P.R. China
E-mail: qingyong@scu.edu.cn

*Contributed equally

Abbreviations: APG, apigenin; DSB, DNA double-strand break; CAs, chromosomal aberrations; HR, homologous recombination; CPT, camptothecin; Top1, topoisomerase I; Top1cc, Top1 covalent protein DNA complex; IR, ionizing radiation; PI, propidium iodide; WT, wild-type

Key words: DNA damage, apigenin, Rad54, homologous recombination

Introduction

Apigenin (APG), a flavonoid widely distributed in a variety of fruits, vegetables and herbs, including oranges, onions and parsley (1), has been demonstrated to be potent against cancer and effective for chemoprophylaxis (2). Its anticancer effects have been examined in multiple cancer types, including breast (3), prostate (4), colon (5) and cervical cancer (6). The anticancer mechanisms of APG are complex. Previous studies demonstrated that APG inhibited the growth of numerous types of cancer cell via inhibition of epidermal growth factor receptor (7-9). APG is also able to induce cell-cycle arrest in G_2/M phase in multiple cell lines (8,10) and trigger apoptosis in leukemia cells (6). APG in combination with tumor necrosis factor-α was able to reduce the cell viability and proliferation of hepatocellular carcinoma cells (11). APG was indicated to target inhibitor proteins of apoptosis in ovarian cancer to induce apoptotic cell death (12). In addition, APG was demonstrated to induce reactive oxygen species and p38, which are essential substances in the process of cell death (7,13,14). Furthermore, it was observed that APG induced DNA lesions involving DNA breaks (15), micronuclei, chromosomal aberrations (CAs) and chromatid exchanges (16-18). APG was further demonstrated to have significant topoisomerase I (Top1) inhibitor activities (19). A previous *in vitro* study demonstrated that APG inhibited the DNA binding or the DNA re-ligation step of Top1 (20).

Induction of DNA lesions is an important mechanism of action of numerous clinical anticancer agents. DNA double-strand breaks (DSBs), the most severe type of DNA lesion, induces cell death if not repaired (21). DSBs were induced by numerous exogenous factors, including ionizing

radiation (IR) (22) and endogenous factors, including topoisomerase (23,24). Camptothecin (CPT), a DNA Top1 inhibitor, has been widely used in the clinic as an anticancer drug. Regarding the mechanism of action, CPT has been demonstrated to selectively bind to and stabilize the 3'phospho-tyrosyl bond formed between Top1 and DNA [Top1 covalent protein DNA complex (Top1cc)] to trap Top1 in Top1cc, which inhibits DNA and RNA synthesis when colliding with the replication fork or transcription machinery to cause DSBs and cell death (25-28). To avoid CPT-induced cell death, two major DNA repair pathways are in place: One is the removal of covalent 3'-DNA adducts by tyrosyl-DNA phosphodiesterase I (TDP1), which hydrolyzes the drug-stabilized 3'phospho-tyrosyl bond of Top1cc (29,30); the other is DSB repair by homologous recombination (HR) (31). Cells deficient of either TDP1 or HR factors, including Rad54, were demonstrated to enhance DNA damage and cell death (32,33).

The DT40 cell line is derived from bursal B-lymphocyte cells (34). It has a stable karyotype and exhibits extraordinarily high gene-targeting efficiency; thus, it has been widely used in genetic studies, including comprehensive research on the mechanisms of DNA damage and repair (35-38). In the present study, the sensitivity to APG, induction of DNA damage and formation of Top1cc were investigated using wild-type (*WT*) DT40 cells, as well as DT40 cells with deletions in several DNA repair genes. The TK6 cell line, a human lymphoblastoid cell line, has numerous advantages, including stable spontaneous mutation frequencies, ability to grow in suspension and simplicity of culture. As a human-derived cell line, TK6 has been widely used for genotoxicity testing (39).

In the present study, it was identified that Rad54, an HR factor, has a critical role in the tolerance to APG-induced DNA damage in DT40 cells. The *Rad54*$^{-/-}$ TK6 cell line was also used to verify these results and it was demonstrated that human Rad54 has the same function in response to APG as that in the chicken DT40 cell line.

Materials and methods

Chemicals. APG and CPT were purchased from MedChemExpress. APG (50 mM) and CPT (100 μM) were prepared and stored at -20˚C. The chemicals were dissolved with DMSO to produce stock solutions.

Cell culture. DT40 cells and human lymphoblast TK6 cells were provided by Dr Shunichi Takeda (Department of Radiation Genetics, Graduate School of Medicine, Kyoto University, Kyoto, Japan; Table I). DT40 cells were maintained in RPMI-1640 medium (Wisent, Inc.) containing 10% heat-inactivated FBS (Wisent, Inc.), 1% chicken serum (Gibco; Thermo Fisher Scientific, Inc.), 1% penicillin-streptomycin (Wisent, Inc.) and 50 μM β-mercaptoethanol (Gibco; Thermo Fisher Scientific, Inc.). The medium for TK6 cells was RPMI-1640, supplemented with 10% heat-inactivated horse serum (HyClone; Cytiva) and 1% penicillin-streptomycin. All cell lines were maintained at 37˚C in a humidified atmosphere with 5% CO_2.

Cell viability assay. The cells were exposed to APG (0, 10, 20 and 30 μM) and CPT (0, 10, 20, 30 and 40 nM) for 72 h, and subsequently, 20 μl Cell Counting Kit-8 (CCK-8; MedChemExpress) reagent was added to each well. The absorbance of each well was measured at 450 nm using a microplate reader (SynergyMx; BioTek Instruments, Inc.). Cell survival curves were constructed from the CCK-8 assay as previously described (40). SPSS software version 20.0 (IBM Corp.) was used to calculate the survival percentage compared with the control. Relative IC_{50} value = (The IC_{50} of deletion cells/The IC_{50} of *WT* cells) x100%.

Cell-cycle assays. Flow cytometry was used to determine cell-cycle arrest (41). In total, $4x10^5$ cells were cultured with 20 μM APG or 6 nM CPT for 16 h. Subsequently, the cells were fixed with 70% ethanol for 4˚C overnight prior to staining with propidium iodide (PI) in the presence of RNase A (cat. no. ST579; Beyotime Institute of Biotechnology) (42). The results were determined using a flow cytometer (CytoFLEX; Beckman Coulter, Inc.).

Colony formation assay. The colony formation assay was performed as previously described (39,43). The medium for DT40 cells included various amounts of APG, mixed with DMEM-F12 (Gibco; Thermo Fisher Scientific, Inc.) supplemented with 15% heat-inactivated FBS (Wisent, Inc.), 1.5% chicken serum (Wisent, Inc.), 1.5% (w/v) methylcellulose, 200 mM L-glutamine (Gibco; Thermo Fisher Scientific, Inc.) and 50 μM β-mercaptoethanol (Gibco; Thermo Fisher Scientific, Inc.) using a slowly rotating shaker overnight at 4˚C. The medium for TK6 cells contained various amounts of drugs, which were mixed with 1.5% (w/v) methylcellulose medium containing 10% heat-inactivated horse serum using slowly rotating tubes overnight at 4˚C. Cells (100 cells/well) were seeded into six-well plates containing 3 ml methylcellulose medium per well and after 14 days, visible white colonies were counted in each well.

Immunofluorescence staining and image analysis. Immunofluorescence staining was performed as previously described (43). In total, $5x10^5$ cells were treated with 30 μM APG or 100 nM CPT for 3, 6 and 9 h. The cells were then fixed with 4% paraformaldehyde for 10 min at room temperature. After washing with PBS, the cells were permeabilized with 0.1% Nonidet P-40. The cells were then blocked with PBS containing 3% BSA (cat. no. A8020; Beijing Solarbio Science & Technology Co., Ltd.) at room temperature for 30 min and incubated with a mouse monoclonal γ-phosphorylated H2A.X variant histone (γ-H2AX; Ser139) antibody (1:1,000; cat. no. 05-636; EMD Millipore) at 4˚C overnight. Anti-mouse Alexa Fluor 488-conjugated antibody (1:1,000; cat. no. A0216; Beyotime Institute of Biotechnology) was used as the secondary antibody at 37˚C for 1 h. The γ-H2AX foci were visualized under a fluorescent microscope (AX10 imager A2/AX10 Cam HRC; Zeiss). The nuclei were stained with DAPI for 10 min at room temperature. The foci of 100 nuclei were counted per well as described in previous reports using Photoshop (version 12.0.3; Adobe Systems, Inc.) (39,43). Experiments were performed three times independently.

Detection of CAs. Karyotype analysis was performed according to a previous study (44). In brief, cells were treated with APG or CPT for different durations. At 3 h prior to harvesting, 0.2 μg/ml colchicine solution (Gibco; Thermo Fisher Scientific,

Table I. DNA repair genes mutated in the DT40 and TK6 clones analyzed.

Gene	Name of cell line	Function	Reference
Fen1	Chicken DT40	Base excision repair, processing 5'flap in long-patch and lagging strand DNA	(48)
Rad18	Chicken DT40	TLS	(49)
Parp1	Chicken DT40	Poly(ADP) ribosylation, related to single-strand break and BER	(50)
Rad54	Chicken DT40	DSB repair by HR	(51)
Rad54	Human TK6	DSB repair by HR	(53)
TDP1	Human TK6	Tyrosyl-DNA phosphodiesterase I	(54)

TLS, translesion DNA synthesis; HR, homologous recombination; BER, base excision repair; DSB, double-strand break; TDP1, tyrosyl-DNA phosphodiesterase 1; PARP1, poly(ADP-ribose) polymerase; FEN1, flap structure-specific endonuclease 1; ADP, adenosine diphosphate.

Inc.) was added. The suspended cells were incubated in 75 mM KCl solution for 25 min and then fixed in Carnoy's solution. The cell suspension was dripped onto ethanol-soaked glass slides and dried using a flame. The dried slides were stained with 5% Giemsa solution and rinsed with water.

In vitro complex of enzyme (ICE) assay. Top1-DNA adducts were isolated using the ICE Bio-assay as described in a previous study (36). In total, $1.5x10^7$ cells per sample were treated with APG or CPT and then suspended in 2 ml buffer A (10 mM HEPES, 10 mM KCl, 1.5 mM $MgCl_2$, 0.34 M sucrose, 10% glycerol, 0.1% Triton X-100; 1 mM phenylmethylsulfonyl fluoride) and put on ice for 10 min. The precipitate was then resuspended in 2 ml buffer B (2 mM EDTA, 0.3 mM egtazic acid, 0.1% Triton X-100 and protease inhibitor) and incubated for 30 min on ice. The chromatin sediment was washed with buffer C (25 mM Tris-Cl, 300 mM NaCl, 10% glycerol and protease inhibitor) five times. After being resuspended in 2 ml 6 M guanidinium chloride, DNA solutions were loaded onto the top of a cushion of CsCl (densities of CsCl solutions: 1.82, 1.7, 1.5 and 1.45 g/ml) and samples were centrifuged at 100,000 x g for 16 h at room temperature. Subsequently, 1 ml supernatant of each part was collected. For dot blot analysis, 100 μl of each fraction was loaded onto a Bio-Dot apparatus (cat. no. 1706545; Bio-Rad Laboratories, Inc.). After washing with Tris-buffered saline with Tween-20, the membrane was incubated with anti-Top1 antibody at 4˚C for 24 h (1:10,000; cat. no. ab109374; Abcam) for 24 h and subsequently incubated with an anti-rabbit antibody conjugated with horseradish peroxidase at 37˚C for 1 h (1:1,000; cat. no. A0208; Beyotime Institute of Biotechnology).

Statistical analysis. Statistical significance of differences was examined using Student's t-test or two-way analysis of variance with Bonferroni's test. Statistical analysis was performed with SPSS 25.0 software (IBM Corp.). $P<0.05$ was considered to indicate a statistically significant difference.

Results

$Rad54^{-/-}$ DT40 cells are sensitized to APG. DT40 chicken B-lymphocyte cells (45) have been widely used in research on DNA lesions and repair (46,47). To examine the molecular mechanisms of APG-induced DNA lesions and their repair, the effects of APG on the viability of *WT* DT40 cells, as well as DT40 cells deletions in several DNA repair genes, flap structure-specific endonuclease 1 ($FEN1)^{-/-}$ (48), $Rad18^{-/-}$ (49), poly(ADP-ribose) polymerase 1 ($PARP1)^{-/-}$ (50) and $Rad54^{-/-}$ (51), were studied and compared. Those cells were separately defective in several DNA repair pathways (Table I). Cells were treated with different concentrations of APG for 72 h and a CCK-8 assay was used to determine their viability. The 50% inhibitory concentration was calculated using SPSS 20.0 software (IBM Corp.). As presented in Fig. 1A and B, $Rad54^{-/-}$ cells deficient of HR repair demonstrated significant sensitivity to APG, while the cells deficient in other DNA repair pathways, were not sensitive to APG. The sensitivity of $Rad54^{-/-}$ cells to APG was also demonstrated in the colony formation assay, as presented in Figs. 1C and S1A. CPT, a Top1 inhibitor, which has been previously demonstrated to sensitize $Rad54^{-/-}$ DT40 cells (52), was used as the positive control, as presented in Fig. 1D.

APG treatment leads to G_2/M-phase cell-cycle arrest of $Rad54^{-/-}$ DT40 cells. Changes in the cell cycle of $Rad54^{-/-}$ DT40 cells compared with *WT* cells were determined. After 16 h of APG treatment, flow cytometric analysis of PI-stained cells demonstrated that the *WT* and $Rad54^{-/-}$ cells were arrested at the G_2/M phase of the cell cycle. Furthermore, APG led to a higher degree of accumulation of in the G_2/M phase for $Rad54^{-/-}$ cells compared with that in *WT* cells. CPT also promoted G_2/M-phase arrest of $Rad54^{-/-}$ cells (Fig. 2).

APG treatment produces more DSBs in $Rad54^{-/-}$ DT40 cells. To verify the effect of APG to induce DNA damage in DT40 cells, the APG-induced γ-H2AX foci in DT40 cells were quantified. DT40 *WT* and $Rad54^{-/-}$ cells were treated with 30 μM APG for 0, 3, 6 and 9 h. As presented in Figs. 3A and S2A, the numbers of γ-H2AX foci were significantly increased in the nuclei and peaked at 6 h after APG exposure in both *WT* and $Rad54^{-/-}$ cells. However, in the $Rad54^{-/-}$ cells, γ-H2AX foci increased more significantly in response to APG (Figs. 3A and S2A) or CPT treatment (Figs. 3B and S2A). The patterns of γ-H2AX foci induced by APG and CPT in $Rad54^{-/-}$ cells were similar.

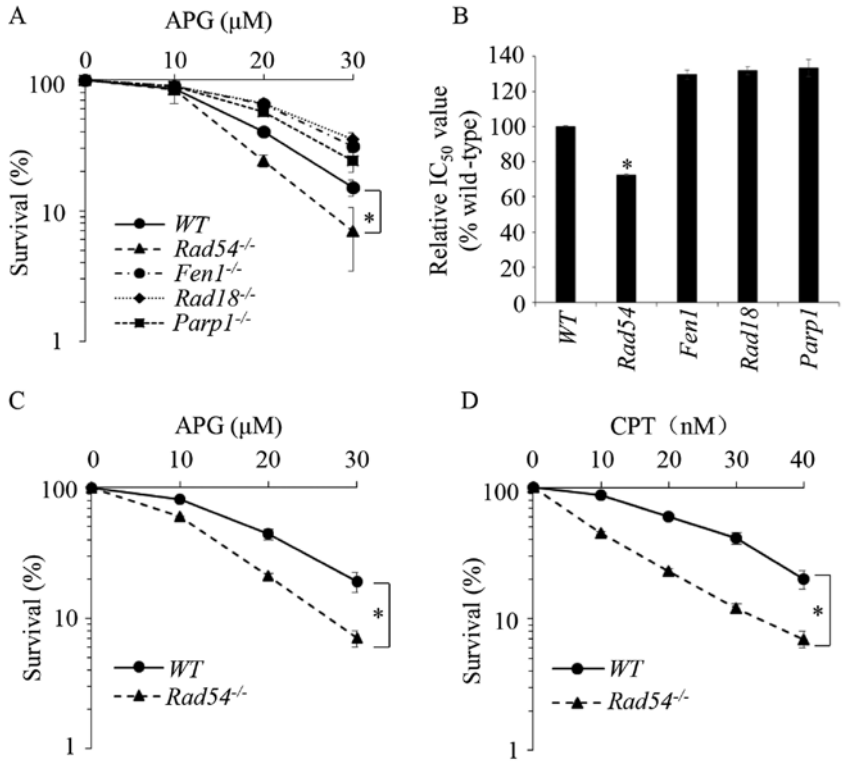

Figure 1. *Rad54*$^{-/-}$ cells are sensitized to APG. (A) Sensitivity of *Parp1*$^{-/-}$, *Rad18*$^{-/-}$, *Fen1*$^{-/-}$ and *Rad54*$^{-/-}$ cells to APG. The x-axis represents the concentration of APG and the y-axis represents the relative percentage of cell survival at 72 h. Two-way analysis of variance with Bonferroni's test was used to test for differences in the linear dose-response curves between *WT* and mutant cells. *P<0.01 *WT* vs. *Rad54*$^{-/-}$ cells; *WT* vs. *Parp1*$^{-/-}$ cells; *WT* vs. Rad18$^{-/-}$ cells; *WT* vs. *Fen1*$^{-/-}$ cells. (B) Relative IC_{50} values of APG in DT40 cells. The x-axis represents the DT40 cells and the y-axis represents the relative number of surviving cells at 72 h. IC_{50} is the concentration at which APG reduces cellular survival to 50% relative to cellular survival without APG treatment. The IC_{50} was calculated from the results of CCK-8 survival assay. Proliferative ability of (C) APG- and (D) CPT-treated DT40 cells determined by clonogenic assays. The x-axis represents the concentration of drugs and the y-axis represents the fractions of surviving colonies on a logarithmic scale. Survival data were log-transformed to approximate normality. Values are expressed as the mean ± standard deviation. The experiments were performed three times independently. Two-way analysis of variance was used to test for differences in the linear dose-response curves between *WT* cells and deletion cells. *P<0.05, control vs. *Rad54*$^{-/-}$ cells. APG, apigenin; CPT, camptothecin; *WT*, wild-type; PARP1, poly(ADP-ribose) polymerase; FEN1, flap structure-specific endonuclease 1; ADP, adenosine diphosphate.

However, compared with the *WT*, the increase of CPT-induced γ-H2AX foci in *Rad54*$^{-/-}$ cells was significantly greater than that induced by APG at 9 h.

APG-induced DSBs in *Rad54*$^{-/-}$ cells were also compared with the *WT* by measuring CAs in DT40 cells. Cells were incubated with 20 μM APG or 10 nM CPT and CAs were confirmed dynamically at 8, 16 and 24 h. The largest number of CAs was counted after 16 h of treatment with APG (Fig. 4A and B) or CPT (Fig. 4C). As presented in Fig. 4, *Rad54*$^{-/-}$ cells had significantly increased numbers of CAs than *WT* cells in response to APG or CPT treatment. These results suggested that Rad54 participated in repairing APG-induced DNA damage.

APG traps Top1cc in Rad54$^{-/-}$ *DT40 cells*. It was then was further assessed whether APG induced Top1cc in DT40 cells. Cells were lysed and Top1cc was separated from free Top1 in the cellular lysates by subjecting cellular extract to CsCl gradient ultracentrifugation. Free Top1 remained in the top two fractions, while Top1cc moved to lower fractions of the CsCl gradient corresponding to the migration of chromosomal DNA. DT40 cells were cultivated with 100 μM APG or CPT for 2 h and an ICE assay was used to detect Top1cc and free Top1. As presented in Fig. 5, fractions 1-2 were mainly free protein and Top1cc peaked at fraction 3. The results in Fig. 5 demonstrated that both APG and CPT induced more accumulation of Top1cc in *Rad54*$^{-/-}$ cells than in *WT* cells (Fig. 5). This observation suggested that APG is able to trap Top1 to remain in a covalent protein-DNA complex in DT40 cells, suggesting that APG is a Top1 inhibitor.

APG induces sensitivity and increases DSBs and Top1cc in Rad54$^{-/-}$ *and TDP1*$^{-/-}$ *TK6 cells*. In order to identify whether human Rad54 was also involved in tolerance of DNA lesions induced by APG, the effects of APG in *Rad54*$^{-/-}$ TK6 cells were studied and compared (53). As presented in Figs. 6A and B, and S1B, *Rad54*$^{-/-}$ TK6 cells were more sensitive to APG or CPT than *WT* cells in the colony formation assay. Following treatment with 80 μM APG or 20 nM CPT for 0, 3, 6 and 9 h, the number of γ-H2AX foci in *Rad54*$^{-/-}$ TK6 cells was significantly increased as compared with that in *WT* TK6 cells (Figs. 6C and D, and S2B). Furthermore, Top1cc was observed in TK6 cells after treatment with 100 μM APG or 2 nM CPT for 2 h, and the drugs induced increased Top1cc in *Rad54*$^{-/-}$ compared with *WT* cells (Fig. 6E). These data were consistent with the results obtained with DT40 cells, suggesting that APG may be a human Top1 inhibitor, which may induce Rad54-dependent tolerance of DNA damage.

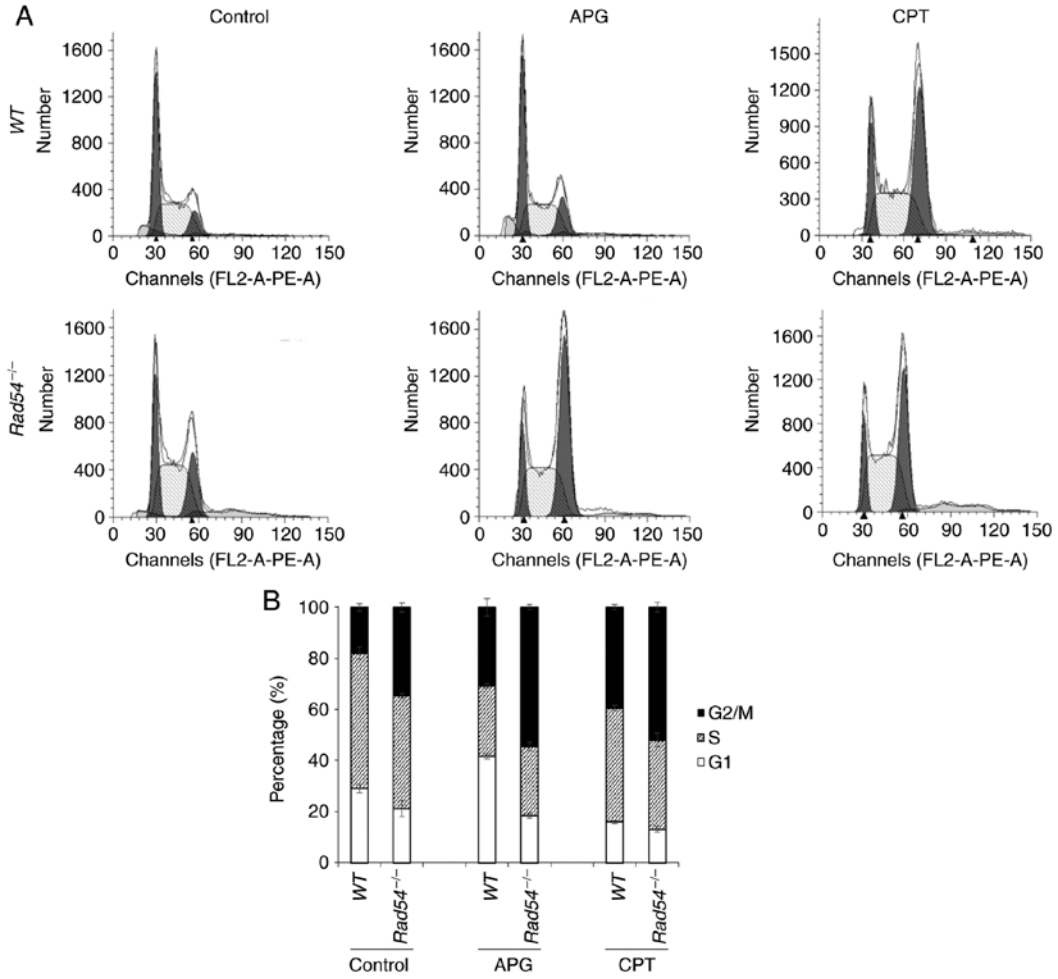

Figure 2. APG induces cell-cycle arrest in G_2/M phase. (A) Representative results demonstrating that APG induced cell-cycle arrest in DT40 cells. DT40 cells were treated with 20 μM APG or 6 nM CPT for 16 h. The cells were then subjected to cell-cycle analysis. (B) Quantitative analysis of the cell-cycle results. Values are expressed as the mean ± standard deviation. Experiments were performed three times independently. APG, apigenin; CPT, camptothecin; *WT*, wild-type.

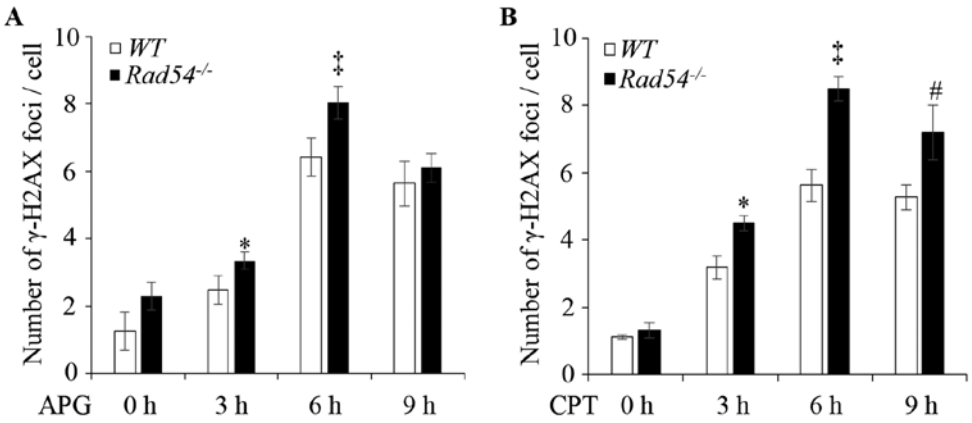

Figure 3. APG induces accumulation of γ-H2AX in nuclei of DT40 cells. (A) Quantification of γ-H2AX foci in *WT* and *Rad54*$^{-/-}$ cells after treatment with 30 μM APG. (B) Quantification of γ-H2AX foci in *WT* and *Rad54*$^{-/-}$ cells after treatment with 100 nM CPT. *WT* and *Rad54*$^{-/-}$ cells were treated for 0, 3, 6 and 9 h. At least 100 cells were analyzed for each data-point. γ-H2AX foci were visualized under a fluorescent microscope (AX10 imager A2/AX10 Cam HRC). Values are expressed as the mean ± standard deviation. Experiments were performed three times independently. *P<0.05, treatment for 3 h compared with *WT*; ‡P<0.05, treatment for 6 h compared with *WT*; $^{\#}$P<0.05, compared with *WT* after the treatment for 9 h. APG, apigenin; CPT, camptothecin; *WT*, wild-type; γ-H2AX, γ-phosphorylated H2A.X variant histone.

Based on the function of TDP1 in Top1-associated DNA damage repair by hydrolyzing the 3' phospho-tyrosyl bond of Top1cc (54,55), it was hypothesized that cells deficient in TDP1 should also be sensitive to APG. Therefore, the cytotoxic effects in *TDP1*$^{-/-}$ TK6 cells were investigated after treating cells with different concentrations of APG (0, 10, 20 and 30 μM) and

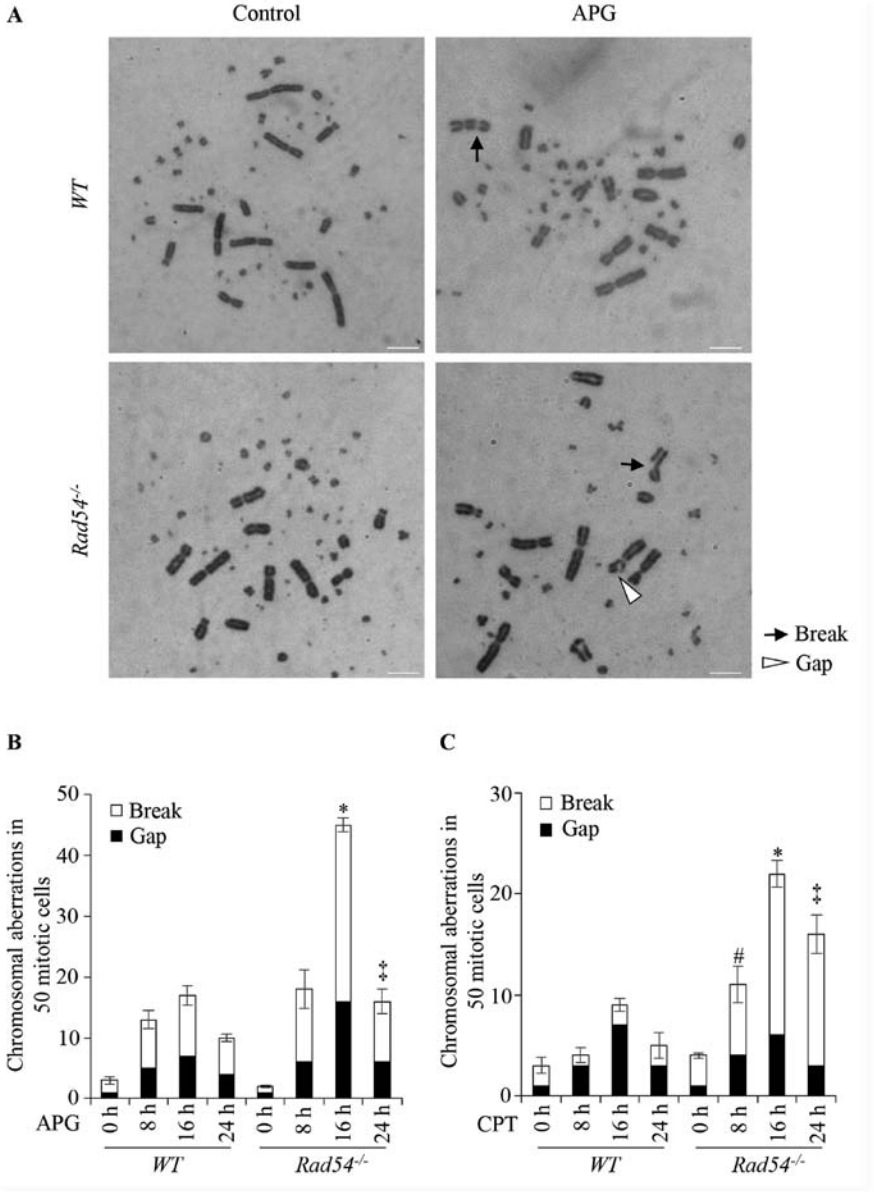

Figure 4. APG induces double-strand breaks in DT40 cells. (A) Representative karyotype analysis of untreated DT40 cells and cells treated with 20 μM APG. Magnification, x1,000. Black arrows indicate breaks whereas white arrowheads indicate gaps. (B) CAs in *WT* and *Rad54*$^{-/-}$ cells after treatment with APG (20 μM) for 8-24 h. (C) CAs in *WT* and *Rad54*$^{-/-}$ cells after treatment with CPT (10 nM) for 8-24 h. In total, 50 metaphase cells per each experiment were analyzed under a light microscope (magnification, x1,000). Values are expressed as the mean ± standard deviation. Experiments were performed three times independently. $^{\#}$P<0.05, total number of breaks and gaps in *Rad54*$^{-/-}$ cells compared with *WT* DT40 cells after treatment for 8 h; *P<0.05, total number of breaks and gaps in *Rad54*$^{-/-}$ cells compared with *WT* DT40 cells after treatment for 16 h; ‡P<0.05, total number of breaks and gaps compared with *WT* DT40 cells after treatment for 24 h. APG, apigenin; CAs, chromosomal aberrations; CPT, camptothecin; *WT*, wild-type.

CPT (0, 2, 4, 6 and 8 nM) for 72 h. The results suggested that *TDP1*$^{-/-}$ TK6 cells were more sensitive to APG than *WT* cells with similar effects of CPT in the colony formation assay (Figs. S1B and S3A and B). Subsequently, the effects of APG-induced DNA-damage on *TDP1*$^{-/-}$ cells were examined. *WT* and *TDP1*$^{-/-}$ TK6 cells were treated with 80 μM APG or 20 nM CPT for 0, 3, 6 and 9 h. The results indicated that the numbers of γ-H2AX foci in the nuclei were significantly increased and peaked at 6 h after APG exposure in *WT* and *TDP1*$^{-/-}$ TK6 cells. In *TDP1*$^{-/-}$ TK6 cells, γ-H2AX foci were increased more significantly in response to APG or CPT treatment compared with those in *WT* cells (Figs. S2B and S3C and D). These results suggested that APG or CPT induced more DNA damage in *TDP1*$^{-/-}$ TK6 cells. Furthermore, Top1cc was observed in *TDP1*$^{-/-}$ TK6 cells after treatment with 100 μM APG or 2 nM CPT for 2 h, and the results demonstrated that APG or CPT induced more Top1cc in *TDP1*$^{-/-}$ TK6 cells than in *WT* cells (Fig. S3E). These results further suggested that APG is a Top1 inhibitor, which is able to trap Top1 in Top1cc, and increased Top1cc was observed in *TDP1*$^{-/-}$ vs. *WT* cells.

Discussion

It has been demonstrated that APG possesses a series of biological effects, including antiviral, antibacterial, antioxidant, anti-inflammatory and anticancer effects (3,56-59). APG was also indicated to cause DNA lesions (60,61). In the present study, DT40 cells with deletions of various DNA damage repair genes

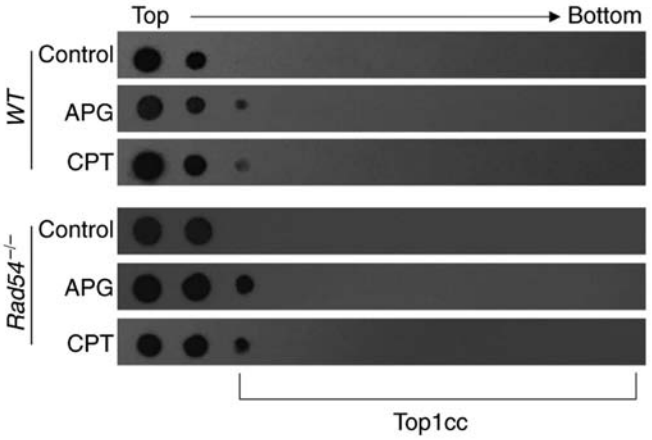

Figure 5. APG causes the formation of Top1cc in DT40 cells. APG treatment of DT40 cells induced the formation of Top1cc. DT40 cells were treated with 100 μM APG or 5 μM CPT for 2 h. Experiments were performed three times independently. In the dot blot, top to bottom indicates the order in which the fractions were taken out of the sample after ultracentrifugation. APG, apigenin; Top1cc, topoisomerase I covalent protein DNA complex; CPT, camptothecin; *WT*, wild-type.

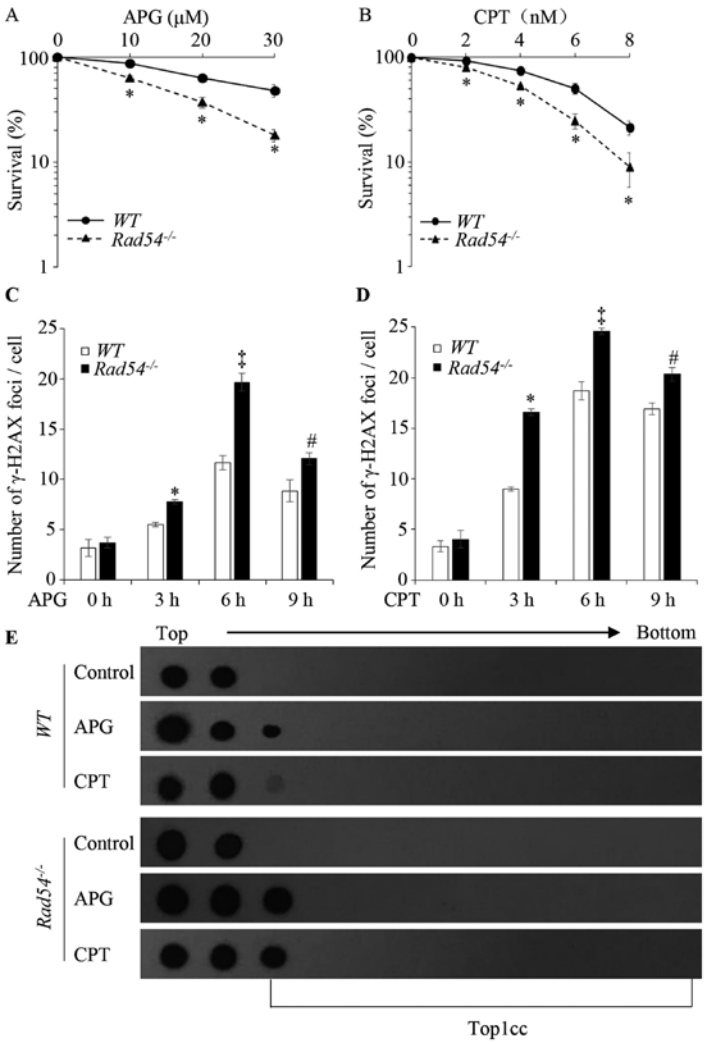

Figure 6. Effects of APG on the proliferative ability and DNA damage in *Rad54*$^{-/-}$ TK6 cells. Proliferative ability of (A) APG- and (B) CPT-treated TK6 cells determined by clonogenic assays. The x-axis represents the concentration of the drugs and the y-axis represents the fractions of surviving colonies on a logarithmic scale. Survival data were log-transformed to approximate normality. Two-way analysis of variance was used to test for differences in the linear dose-response curves between *WT* and *Rad54*$^{-/-}$ cells. *P<0.05, *Rad54*$^{-/-}$ cells compared with *WT*. (C) Quantification of γ-H2AX foci in *WT* and *Rad54*$^{-/-}$ cells after treatment with 80 μM APG. (D) Quantification of γ-H2AX foci in *WT* and *Rad54*$^{-/-}$ cells after treatment with 20 nM CPT. TK6 cells were treated for 0, 3, 6 and 9 h, respectively; 100 cells were analyzed for each data-point. (E) APG induced the formation of Top1cc in TK6 cells. TK6 cells were treated with 100 μM APG and 2 μM CPT for 2 h to detect Top1cc. In the dot blot, top to bottom indicates the order in which the fractions were taken out of the sample after ultracentrifugation. Values are expressed as the mean ± standard deviation. Experiments were performed three times independently. *P<0.05, compared with *WT* after treatment for 3 h; ‡P<0.05, compared with *WT* after treatment for 6 h; $^{\#}$P<0.05, compared with *WT* after treatment for 9 h. APG, apigenin; CPT, camptothecin; *WT*, wild-type; γ-H2AX, γ-phosphorylated H2A.X variant histone; Top1cc, topoisomerase I covalent protein DNA complex.

were used to examine the possible molecular mechanisms of APG-induced DNA damage repair, and it was identified that *Rad54*$^{-/-}$ DT40 cells were specifically sensitive to APG. The cell-cycle assay demonstrated that APG also induced more cell-cycle arrest in G_2/M phase in *Rad54*$^{-/-}$ than in *WT* cells.

Rad54 is the most highly conserved eukaryotic HR protein, which is involved in various activities that contribute to the progression of HR (62). The Rad54 protein is part of a nucleoprotein filament to confer DNA homology (63,64). It interacts with the Rad51 nucleoprotein filament and induces the activity of DNA pairing in HR (51). HR is an important DNA repair pathway for DSBs. It repairs DSBs in the S phase (62). It was demonstrated that lack of Rad54 in DT40 cells leads to sensitivity to endogenous factors, including topoisomerase (65), and exogenous factors, such as IR (66), which is able to induce DSBs in the S-phase (67,68). In the present study, *Rad54*$^{-/-}$ DT40 cells were sensitive to APG, demonstrating that APG may induce DSBs that are tolerated in the presence of Rad54. Cell-cycle arrest is an important cell response to DNA lesions that is initiated by activating cell-cycle checkpoint proteins. It was previously demonstrated that APG caused arrest of the cell cycle in G_0/G_1-phase by reducing the level of cyclin D1 in LNCaP and PC-3 prostate cancer cell lines (1). However, in other studies, APG caused cell-cycle arrest at the G_2-phase by decreasing cyclin B in human colon carcinoma and pancreatic cancer cells (10), or regulated other cell-cycle phases by affecting cyclin A and cell division cycle 25A and cell division cycle 25C in different cell types (8,69-71). The results of the cell-cycle assay of the present study suggested that APG arrested *Rad54*$^{-/-}$ cells in G_2/M-phase. To identify whether APG induced DSBs, the γ-H2AX foci were quantified as a marker for DSBs and CAs representing stable DSBs were also evaluated. Analysis of both γ-H2AX foci and CAs identified that APG induced increased DSBs in *Rad54*$^{-/-}$ cells compared with the *WT* cells. The results suggested that the enhanced sensitivity and increased amount of cell-cycle arrest of *Rad54*$^{-/-}$ cells in G_2/M-phase were associated with the induction of DSBs by APG.

HR has been identified as the essential Top1-associated repair pathway for DSBs (72). Numerous flavonoids, including APG, quercetin, kaempferol and morin, have been identified as Top1 inhibitors (20,73). Previous studies (20,73) reported that several flavonoids, including APG, were similar to CPT and were able to stabilize Top1cc *in vitro* and *in vivo*. Consistent with these previous studies, the present study demonstrated that APG induced significant Top1cc formation in *Rad54*$^{-/-}$ cells. Furthermore, human *Rad54*$^{-/-}$ TK6 cells exhibited the same sensitivities to APG and increased DSBs and Top1cc formation as *Rad54*$^{-/-}$ DT40 cells. These results suggested that APG may be a Top1 inhibitor, which traps Top1 in the form of Top1cc. When Top1cc encounters a replication fork, it leads to cell-cycle arrest and even DSBs, which is mainly repaired by HR. Lack of Rad54 affects the repair of DSBs caused by the sustained existence of Top1cc.

Top1 is an important enzyme for DNA replication, transcription, recombination and chromatin remodeling, which relaxes the supercoil structure of DNA molecules by cutting one strand of duplex DNA and generating Top1cc that causes supercoiled DNA to untwist (74). Under physiological conditions, Top1cc is resolved by TDP1, which catalyzes hydrolysis of the Top1 tyrosine residue covalently linked to the 3'-phosphate of DNA, removes Top1 from the DNA 3'-end so that the broken DNA strand is religated (75). A previous study has demonstrated that deficiency of TDP1 leads to accumulation of Top1cc and DSBs, and a Top1 inhibitor, e.g. CTP, was able to enhance accumulation of Top1cc and DSBs (76). In the present study, it was identified that TK6 cells deficient of TDP1 were also sensitive to APG, which generated increased DSBs and Top1cc. This result further suggested that APG is a Top1 inhibitor.

To the best of our knowledge, the present study was the first to examine the role of Rad54 in the tolerance of APG-induced Top1-mediated DNA damage by using DNA repair-deficient DT40 and TK6 cells. The data suggested that inhibition of Rad54 may enhance the toxicity of APG to tumor cells. The present results also suggested that APG-induced toxicity was enhanced by Rad54 deletion, such that Rad54 may be included in the potential DNA rearrangements caused by APG for the treatment of other diseases. The present study provided insight for developing novel anticancer medicines with higher therapeutic efficacy and less genotoxicity.

Acknowledgements

The authors would like to thank Dr Hiroyuki Sasanuma (Department of Radiation Genetics, Graduate School of Medicine, Kyoto University, Koyot, Japan) for providing the complete protocol of *in vitro* complex of enzyme analysis.

Funding

The present study was supported by the Fundamental Research Funds for the Central Universities and The 111 Project (grant no. B18035).

Availability of data and materials

All data generated or analyzed during the present study are included in this published article.

Authors' contributions

YQ, XW, FH and ZZ conceived and designed the experiments. ZZ and CX performed the experiments. ZZ, YQ, XW, FH, CX, XF and XL analyzed the data. ZZ, YQ, XW, CX, JZ and XB contributed reagents/materials/analysis tools. ZZ, XW and YQ wrote the manuscript. ST was responsible for the generation of gene knock-out cells. XB and JZ developed the method for the ICE assay, verified the results and ensured that the results could be reproduced. All authors read and approved the final manuscript.

Ethics approval and consent to participate

Not applicable.

Patient consent for publication

Not applicable.

Competing interests

The authors declare that they have no competing interests.

References

1. Shukla S, Bhaskaran N, Babcook MA, Fu P, Maclennan GT and Gupta S: Apigenin inhibits prostate cancer progression in TRAMP mice via targeting PI3K/Akt/FoxO pathway. Carcinogenesis 35: 452-460, 2014.
2. Tong X and Pelling JC: Targeting the PI3K/Akt/mTOR axis by apigenin for cancer prevention. Anticancer Agents Med Chem 13: 971-978, 2013.
3. Perrott KM, Wiley CD, Desprez PY and Campisi J: Apigenin suppresses the senescence-associated secretory phenotype and paracrine effects on breast cancer cells. Geroscience 39: 161-173, 2017.
4. Shukla S, Kanwal R, Shankar E, Datt M, Chance MR, Fu P, MacLennan GT and Gupta S: Apigenin blocks IKKα activation and suppresses prostate cancer progression. Oncotarget 6: 31216-31232, 2015.
5. Shao H, Jing K, Mahmoud E, Huang H, Fang X and Yu C: Apigenin sensitizes colon cancer cells to antitumor activity of ABT-263. Mol Cancer Ther 12: 2640-2650, 2013.
6. Souza RP, Bonfim-Mendonça PS, Gimenes F, Ratti BA, Kaplum V, Bruschi ML, Nakamura CV, Silva SO, Maria-Engler SS and Consolaro ME: Oxidative stress triggered by apigenin induces apoptosis in a comprehensive panel of human cervical cancer-derived cell lines. Oxid Med Cell Longev 2017: 1512745, 2017.
7. Yin F, Giuliano AE, Law RE and Van Herle AJ: Apigenin inhibits growth and induces G2/M arrest by modulating cyclin-CDK regulators and ERK MAP kinase activation in breast carcinoma cells. Anticancer Res 21: 413-420, 2001.
8. Wang W, Heideman L, Chung CS, Pelling JC, Koehler KJ and Birt DF: Cell-cycle arrest at G2/M and growth inhibition by apigenin in human colon carcinoma cell lines. Mol Carcinog 28: 102-110, 2000.
9. Caltagirone S, Rossi C, Poggi A, Ranelletti FO, Natali PG, Brunetti M, Aiello FB and Piantelli M: Flavonoids apigenin and quercetin inhibit melanoma growth and metastatic potential. Int J Cancer 87: 595-600, 2000.
10. Ujiki MB, Ding XZ, Salabat MR, Bentrem DJ, Golkar L, Milam B, Talamonti MS, Bell RH Jr, Iwamura T and Adrian TE: Apigenin inhibits pancreatic cancer cell proliferation through G2/M cell cycle arrest. Mol Cancer 5: 76, 2006.
11. Chen Z, Chen J, Liu H, Dong W, Huang X, Yang D, Hou J and Zhang X: The SMAC mimetic APG-1387 sensitizes immune-mediated cell apoptosis in hepatocellular carcinoma. Front Pharmacol 9: 1298, 2018.
12. Li BX, Wang HB, Qiu MZ, Luo QY, Yi HJ, Yan XL, Pan WT, Yuan LP, Zhang YX, Xu JH, *et al*: Novel smac mimetic APG-1387 elicits ovarian cancer cell killing through TNF-alpha, Ripoptosome and autophagy mediated cell death pathway. J Exp Clin Cancer Res 37: 53, 2018.
13. Vargo MA, Voss OH, Poustka F, Cardounel AJ, Grotewold E and Doseff AI: Apigenin-induced-apoptosis is mediated by the activation of PKCdelta and caspases in leukemia cells. Biochem Pharmaco 72: 681-692, 2006.
14. Shukla S and Gupta S: Apigenin-induced cell cycle arrest is mediated by modulation of MAPK, PI3K-Akt, and loss of cyclin D1 associated retinoblastoma dephosphorylation in human prostate cancer cells. Cell Cycle 6: 1102-1114, 2007.
15. Meng S, Zhu Y, Li JF, Wang X, Liang Z, Li SQ, Xu X, Chen H, Liu B, Zheng XY, *et al*: Apigenin inhibits renal cell carcinoma cell proliferation. Oncotarget 8: 19834-19842, 2017.
16. Farooqi AA, Wu SJ, Chang YT, Tang JY, Li KT, Ismail M, Liaw CC, Li RN and Chang HW: Activation and inhibition of ATM by phytochemicals: Awakening and sleeping the guardian angel naturally. Arch Immunol Ther Exp (Warsz) 63: 357-366, 2015.
17. Noel S, Kasinathan M and Rath SK: Evaluation of apigenin using in vitro cytochalasin blocked micronucleus assay. Toxicol In Vitro 20: 1168-1172, 2006.
18. Papachristou F, Chatzaki E, Petrou A, Kougioumtzi I, Katsikogiannis N, Papalambros A, Tripsianis G, Simopoulos C and Tsaroucha AK: Time course changes of anti- and pro-apoptotic proteins in apigenin-induced genotoxicity. Chin Med 8: 9, 2013.
19. Song J, Parker L, Hormozi L and Tanouye MA: DNA topoisomerase I inhibitors ameliorate seizure-like behaviors and paralysis in a Drosophila model of epilepsy. Neuroscience 156: 722-728, 2008.
20. Boege F, Straub T, Kehr A, Boesenberg C, Christiansen K, Andersen A, Jakob F and Köhrle J: Selected novel flavones inhibit the DNA binding or the DNA religation step of eukaryotic topoisomerase I. J Biol Chem 271: 2262-2270, 1996.
21. Adachi N, Suzuki H, Iiizumi S and Koyama H: Hypersensitivity of nonhomologous DNA end-joining mutants to VP-16 and ICRF-193: Implications for the repair of topoisomerase II-mediated DNA damage. J Biol Chem 278: 35897-35902, 2003.
22. Plante I, Slaba T, Shavers Z and Hada M: A bi-exponential repair algorithm for radiation-induced double-strand breaks: Application to simulation of chromosome aberrations. Genes (Basel) 10: 10, 2019.
23. Morimoto S, Tsuda M, Bunch H, Sasanuma H, Austin C and Takeda S: Type II DNA topoisomerases cause spontaneous double-strand breaks in genomic DNA. Genes (Basel) 10: 10, 2019.
24. Cho JE and Jinks-Robertson S: Deletions associated with stabilization of the Top1 cleavage complex in yeast are products of the nonhomologous end-joining pathway. Proc Natl Acad Sci USA 116: 22683-22691, 2019.
25. Li F, Jiang T, Li Q and Ling X: Camptothecin (CPT) and its derivatives are known to target topoisomerase I (Top1) as their mechanism of action: Did we miss something in CPT analogue molecular targets for treating human disease such as cancer? Am J Cancer Res 7: 2350-2394, 2017.
26. 26. Pommier Y: Drugging topoisomerases: Lessons and challenges. ACS Chem Biol 8: 82-95, 2013.
27. Ji Y, Dang X, Nguyen LN, Nguyen LN, Zhao J, Cao D, Khanal S, Schank M, Wu XY, Morrison ZD, *et al*: Topological DNA damage, telomere attrition and T cell senescence during chronic viral infections. Immun Ageing 16: 12, 2019.
28. Petermann E, Orta ML, Issaeva N, Schultz N and Helleday T: Hydroxyurea-stalled replication forks become progressively inactivated and require two different RAD51-mediated pathways for restart and repair. Mol Cell 37: 492-502, 2010.
29. Borda MA, Palmitelli M, Verón G, González-Cid M and de Campos Nebel M: Tyrosyl-DNA-phosphodiesterase I (TDP1) participates in the removal and repair of stabilized-Top2α cleavage complexes in human cells. Mutat Res 781: 37-48, 2015.
30. Cuya SM, Comeaux EQ, Wanzeck K, Yoon KJ and van Waardenburg RC: Dysregulated human Tyrosyl-DNA phosphodiesterase I acts as cellular toxin. Oncotarget 7: 86660-86674, 2016.
31. Tripathi K, Mani C, Clark DW and Palle K: Rad18 is required for functional interactions between FANCD2, BRCA2, and Rad51 to repair DNA topoisomerase 1-poisons induced lesions and promote fork recovery. Oncotarget 7: 12537-12553, 2016.
32. Yonetani Y, Hochegger H, Sonoda E, Shinya S, Yoshikawa H, Takeda S and Yamazoe M: Differential and collaborative actions of Rad51 paralog proteins in cellular response to DNA damage. Nucleic Acids Res 33: 4544-4552, 2005.
33. Vance JR and Wilson TE: Yeast Tdp1 and Rad1-Rad10 function as redundant pathways for repairing Top1 replicative damage. Proc Natl Acad Sci USA 99: 13669-13674, 2002.
34. Buerstedde JM, Reynaud CA, Humphries EH, Olson W, Ewert DL and Weill JC: Light chain gene conversion continues at high rate in an ALV-induced cell line. EMBO J 9: 921-927, 1990.
35. Buerstedde JM and Takeda S: Increased ratio of targeted to random integration after transfection of chicken B cell lines. Cell 67: 179-188, 1991.
36. Hoa NN, Shimizu T, Zhou ZW, Wang ZQ, Deshpande RA, Paull TT, Akter S, Tsuda M, Furuta R, Tsutsui K, *et al*: Mre11 is essential for the removal of lethal topoisomerase 2 covalent cleavage complexes. Mol Cell 64: 580-592, 2016.
37. Sasanuma H, Tsuda M, Morimoto S, Saha LK, Rahman MM, Kiyooka Y, Fujiike H, Cherniack AD, Itou J, Callen Moreu E, *et al*: BRCA1 ensures genome integrity by eliminating estrogen-induced pathological topoisomerase II-DNA complexes. Proc Natl Acad Sci USA 115: E10642-E10651, 2018.
38. Zong D, Adam S, Wang Y, Sasanuma H, Callén E, Murga M, Day A, Kruhlak MJ, Wong N, Munro M, *et al*: BRCA1 haploinsufficiency is masked by RNF168-mediated chromatin ubiquitylation. Mol Cell 73: 1267-1281.e7, 2019.
39. Liu H, Wu Y, He F, Cheng Z, Zhao Z, Xiang C, Feng X, Bai X, Takeda S, Wu X, *et al*: Brca1 is involved in tolerance to adefovir dipivoxil induced DNA damage. Int J Mol Med 43: 2491-2498, 2019.
40. Zhang Z, Bu X, Chen H, Wang Q and Sha W: Bmi-1 promotes the invasion and migration of colon cancer stem cells through the downregulation of E-cadherin. Int J Mol Med 38: 1199-1207, 2016.
41. Thapa M, Bommakanti A, Shamsuzzaman M, Gregory B, Samsel L, Zengel JM and Lindahl L: Repressed synthesis of ribosomal proteins generates protein-specific cell cycle and morphological phenotypes. Mol Biol Cell 24: 3620-3633, 2013.

42. Lecomte S, Demay F, Pham TH, Moulis S, Efstathiou T, Chalmel F and Pakdel F: Deciphering the molecular mechanisms sustaining the estrogenic activity of the two major dietary compounds zearalenone and apigenin in ER-positive breast cancer cell lines. Nutrients 11: 11, 2019.
43. Hu X, Wu X, Liu H, Cheng Z, Zhao Z, Xiang C, Feng X, Takeda S and Qing Y: Genistein-induced DNA damage is repaired by nonhomologous end joining and homologous recombination in TK6 cells. J Cell Physiol 234: 2683-2692, 2019.
44. Liu Y, Wu X, Hu X, Chen Z, Liu H, Takeda S and Qing Y: Multiple repair pathways mediate cellular tolerance to resveratrol-induced DNA damage. Toxicol In Vitro 42: 130-138, 2017.
45. Baba TW, Giroir BP and Humphries EH: Cell lines derived from avian lymphomas exhibit two distinct phenotypes. Virology 144: 139-151, 1985.
46. Sonoda E, Morrison C, Yamashita YM, Takata M and Takeda S: Reverse genetic studies of homologous DNA recombination using the chicken B-lymphocyte line, DT40. Philos Trans R Soc Lond B Biol Sci 356: 111-117, 2001.
47. Dhar PK, Sonoda E, Fujimori A, Yamashita YM and Takeda S: DNA repair studies: experimental evidence in support of chicken DT40 cell line as a unique model. J Environ Pathol Toxicol Oncol 20: 273-283, 2001.
48. Asagoshi K, Tano K, Chastain PD II, Adachi N, Sonoda E, Kikuchi K, Koyama H, Nagata K, Kaufman DG, Takeda S, *et al*: FEN1 functions in long patch base excision repair under conditions of oxidative stress in vertebrate cells. Mol Cancer Res 8: 204-215, 2010.
49. Yoshinaga N, Shindo K, Matsui Y, Takiuchi Y, Fukuda H, Nagata K, Shirakawa K, Kobayashi M, Takeda S and Takaori-Kondo A: A screening for DNA damage response molecules that affect HIV-1 infection. Biochem Biophys Res Commun 513: 93-98, 2019.
50. Ooka M, Abe T, Cho K, Koike K, Takeda S and Hirota K: Chromatin remodeler ALC1 prevents replication-fork collapse by slowing fork progression. PLoS One 13: e0192421, 2018.
51. Petukhova G, Stratton S and Sung P: Catalysis of homologous DNA pairing by yeast Rad51 and Rad54 proteins. Nature 393: 91-94, 1998.
52. Qing Y, Yamazoe M, Hirota K, Dejsuphong D, Sakai W, Yamamoto KN, Bishop DK, Wu X and Takeda S: The epistatic relationship between BRCA2 and the other RAD51 mediators in homologous recombination. PLoS Genet 7: e1002148, 2011.
53. Takata M, Sasaki MS, Sonoda E, Morrison C, Hashimoto M, Utsumi H, Yamaguchi-Iwai Y, Shinohara A and Takeda S: Homologous recombination and non-homologous end-joining pathways of DNA double-strand break repair have overlapping roles in the maintenance of chromosomal integrity in vertebrate cells. EMBO J 17: 5497-5508, 1998.
54. Al Abo M, Sasanuma H, Liu X, Rajapakse VN, Huang SY, Kiselev E, Takeda S, Plunkett W and Pommier Y: TDP1 is critical for the repair of DNA breaks induced by sapacitabine, a nucleoside also targeting ATM- and BRCA-deficient tumors. Mol Cancer Ther 16: 2543-2551, 2017.
55. Lountos GT, Zhao XZ, Kiselev E, Tropea JE, Needle D, Pommier Y, Burke TR Jr and Waugh DS: Identification of a ligand binding hot spot and structural motifs replicating aspects of tyrosyl-DNA phosphodiesterase I (TDP1) phosphoryl recognition by crystallographic fragment cocktail screening. Nucleic Acids Res 47: 10134-10150, 2019.
56. Sharma H, Kanwal R, Bhaskaran N and Gupta S: Plant flavone apigenin binds to nucleic acid bases and reduces oxidative DNA damage in prostate epithelial cells. PLoS One 9: e91588, 2014.
57. Jayasooriya RG, Kang SH, Kang CH, Choi YH, Moon DO, Hyun JW, Chang WY and Kim GY: Apigenin decreases cell viability and telomerase activity in human leukemia cell lines. Food Chem Toxicol 50: 2605-2611, 2012.
58. Chung CS, Jiang Y, Cheng D and Birt DF: Impact of adenomatous polyposis coli (APC) tumor supressor gene in human colon cancer cell lines on cell cycle arrest by apigenin. Mol Carcinog 46: 773-782, 2007.
59. Gupta S, Afaq F and Mukhtar H: Involvement of nuclear factor-kappa B, Bax and Bcl-2 in induction of cell cycle arrest and apoptosis by apigenin in human prostate carcinoma cells. Oncogene 21: 3727-3738, 2002.
60. Subhasitanont P, Chokchaichamnankit D, Chiablaem K, Keeratichamroen S, Ngiwsara L, Paricharttanakul NM, Lirdprapamongkol K, Weeraphan C, Svasti J and Srisomsap C: Apigenin inhibits growth and induces apoptosis in human cholangiocarcinoma cells. Oncol Lett 14: 4361-4371, 2017.
61. Sharma NK: Modulation of radiation-induced and mitomycin C-induced chromosome damage by apigenin in human lymphocytes in vitro. J Radiat Res (Tokyo) 54: 789-797, 2013.
62. Agarwal S, van Cappellen WA, Guénolé A, Eppink B, Linsen SE, Meijering E, Houtsmuller A, Kanaar R and Essers J: ATP-dependent and independent functions of Rad54 in genome maintenance. J Cell Biol 192: 735-750, 2011.
63. Mazin AV, Alexeev AA and Kowalczykowski SC: A novel function of Rad54 protein. Stabilization of the Rad51 nucleoprotein filament. J Biol Chem 278: 14029-14036, 2003.
64. Mazin AV, Bornarth CJ, Solinger JA, Heyer WD and Kowalczykowski SC: Rad54 protein is targeted to pairing loci by the Rad51 nucleoprotein filament. Mol Cell 6: 583-592, 2000.
65. García-Luis J and Machín F: Fanconi anaemia-like Mph1 helicase nacks up Rad54 and Rad5 to circumvent replication stress-driven chromosome bridges. Genes (Basel) 9: 9, 2018.
66. Tang S, Liu B, Liu M, Li Z, Liu J, Wang H, Wang J, Oh YT, Shen L and Wang Y: Ionizing radiation-induced growth in soft agar is associated with miR-21 upregulation in wild-type and DNA double strand break repair deficient cells. DNA Repair (Amst) 78: 37-44, 2019.
67. Crickard JB, Kaniecki K, Kwon Y, Sung P, Lisby M and Greene EC: Regulation of Hed1 and Rad54 binding during maturation of the meiosis-specific presynaptic complex. EMBO J 37: 37, 2018.
68. Zhang XP, Janke R, Kingsley J, Luo J, Fasching C, Ehmsen KT and Heyer WD: A conserved sequence extending motif III of the motor domain in the Snf2-family DNA translocase Rad54 is critical for ATPase activity. PLoS One 8: e82184, 2013.
69. Zhang L, Cheng X, Gao Y, Zheng J, Xu Q, Sun Y, Guan H, Yu H and Sun Z: Apigenin induces autophagic cell death in human papillary thyroid carcinoma BCPAP cells. Food Funct 6: 3464-3472, 2015.
70. Fang J, Bao YY, Zhou SH and Fan J: Apigenin inhibits the proliferation of adenoid cystic carcinoma via suppression of glucose transporter-1. Mol Med Rep 12: 6461-6466, 2015.
71. Lim W, Park S, Bazer FW and Song G: Apigenin reduces survival of choriocarcinoma cells by inducing apoptosis via the PI3K/AKT and ERK1/2 MAPK pathways. J Cell Physiol 231: 2690-2699, 2016.
72. Nitiss J and Wang JC: DNA topoisomerase-targeting antitumor drugs can be studied in yeast. Proc Natl Acad Sci USA 85: 7501-7505, 1988.
73. Chen G and Guo M: Screening for natural inhibitors of topoisomerases I from Rhamnus davurica by affinity ultrafiltration and high-performance liquid chromatography-mass spectrometry. Front Plant Sci 8: 1521, 2017.
74. Champoux JJ: DNA topoisomerases: Structure, function, and mechanism. Annu Rev Biochem 70: 369-413, 2001.
75. Interthal H, Pouliot JJ and Champoux JJ: The tyrosyl-DNA phosphodiesterase Tdp1 is a member of the phospholipase D superfamily. Proc Natl Acad Sci USA 98: 12009-12014, 2001.
76. Krawczyk C, Dion V, Schär P and Fritsch O: Reversible Top1 cleavage complexes are stabilized strand-specifically at the ribosomal replication fork barrier and contribute to ribosomal DNA stability. Nucleic Acids Res 42: 4985-4995, 2014.